

Designing a cavity-mediated quantum CPHASE gate between NV spin qubits in diamond

Guido Burkard and V. O. Shkolnikov

Department of Physics, University of Konstanz, D-78457 Konstanz, Germany

D. D. Awschalom

Institute for Molecular Engineering, University of Chicago, Chicago, IL 60637, USA

(Received 25 February 2014; revised manuscript received 23 February 2017; published 16 May 2017)

While long spin coherence times and efficient single-qubit quantum control have been implemented successfully in nitrogen-vacancy (NV) centers in diamond, the controlled coupling of remote NV spin qubits remains challenging. Here, we propose and analyze a controlled-phase (CPHASE) gate for the spins of two NV centers embedded in a common optical cavity and driven by two off-resonant lasers. In combination with previously demonstrated single-qubit gates, CPHASE allows for arbitrary quantum computations. The coupling of the NV spin to the cavity mode is based upon Raman transitions via the NV excited states and can be controlled with the laser intensities and relative phase. We find characteristic laser frequencies at which the scattering amplitude of a laser photon into the cavity mode is strongly dependent on the NV center spin. A scattered photon can be reabsorbed by another selectively driven NV center and can generate a conditional phase (CPHASE) gate. Gate times around 200 ns are within reach, nearly two orders of magnitude shorter than typical NV spin coherence times of around 10 μ s. The separation between the two interacting NV centers is limited only by the extension of the cavity.

DOI: [10.1103/PhysRevB.95.205420](https://doi.org/10.1103/PhysRevB.95.205420)

I. INTRODUCTION

Nitrogen-vacancy (NV) centers in diamond have emerged as powerful and versatile quantum systems with applications as sources of nonclassical light, as high-precision sensors, and as qubits for quantum information technology [1]. The electron spin of the NV center unites several essential properties required for quantum information processing (QIP). Its quantum coherence is preserved over long times, even at elevated temperatures, and it allows for optical preparation and readout, as well as quantum gate operations via radio-frequency (rf) excitation, at the level of a single-NV center. One of the remaining challenges on the way towards diamond-based QIP is the establishment of a scalable architecture allowing for the coherent coupling between NV spins. A controlled coupling is required to realize a two-qubit gate such as a controlled-phase (CPHASE) gate or a controlled-NOT (CNOT) gate which forms a universal set of quantum gates in combination with single-qubit gates. Controlled operations between the NV electron spin and a nearby nuclear spin have been performed using a combination of rf and microwave pulses [2], whereas entanglement generation can be achieved between the electron spins of two nearby NV centers on the basis of static dipolar interactions [3] and between NV center spins separated by several meters [4] and subsequently over more than one kilometer [5] via a nondeterministic coincidence measurement protocol. Here, we propose and theoretically analyze a fully controllable and switchable coupling between the spins of distant NV centers coupled to the same mode of a surrounding optical cavity (Fig. 1).

A variety of optical cavity systems for cavity quantum electrodynamics (QED) coupled to defect centers in diamond exists. The advantage of whispering gallery modes of a silica microsphere is their ultrahigh quality factors [6] $Q > 10^8$, whereas photonic crystals fabricated within the diamond crystal [7–9] or on top [10] allow for the embedding of

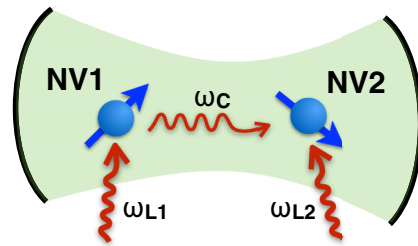


FIG. 1. Two nitrogen-vacancy centers in diamond located in an optical cavity and coupled to a common cavity mode with frequency ω_C (shown schematically). The NV centers are excited by off-resonant laser fields (frequencies ω_{Li}). Spin-dependent scattering of laser photons off the NV center into the cavity mode and back allows for a coupling of the two NV spins which produces the universal CPHASE quantum gate.

the NV centers directly into the optical cavity structure but comprise (so far) somewhat lower Q factors. However, photonic crystal cavities in diamond with $Q > 10^5$ have recently been fabricated [11]. The architecture proposed here can, in principle, be used with any realization of NV-cavity coupling, provided sufficiently high Q and dipole matrix element of the ground-state (GS)-excited-state (ES) transition in the cavity field.

The basic working principle of the quantum gate operation proposed here is as follows. We restrict ourselves to two of the three GS spin-triplet states, $m_s = 0$ and $m_s = -1$, which will serve as the qubit basis in our scheme [Fig. 2(a)]. Near the GS level crossing around a magnetic field of about $B_0 \sim 1000$ G, these two states are nearly degenerate and are separated by several gigahertz from the third ($m_s = +1$) state. Off-resonant coupling of the GS-ES transition to the cavity mode combined with off-resonant laser excitation can be used to generate Raman-type two-photon transitions starting and ending in the GS, accompanied by the scattering of a laser

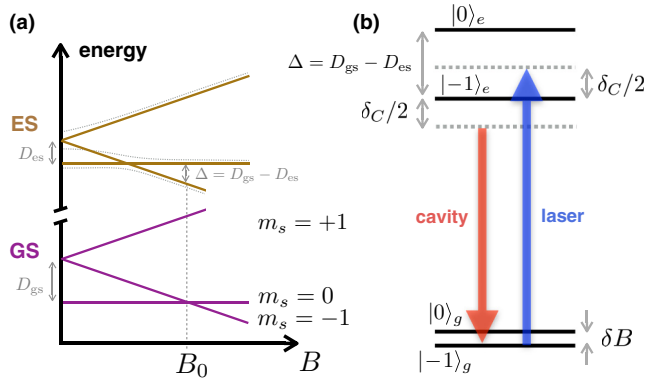


FIG. 2. (a) GS and ES energy levels as a function of the magnetic field B applied along the NV axis. In the ES, only one orbital triplet is shown. The effect of the spin-spin interactions $\Delta_{1,2}$ is shown schematically by the dotted lines. (b) Simplified energy level scheme. Here, $|0\rangle_g$ and $|-1\rangle_g$ denote orbital ground-state levels with spin projections $m_s = 0$ and $m_s = -1$. Similarly, $|0\rangle_e$ and $|-1\rangle_e$ stand for the corresponding excited-state levels. The scattering of a laser photon (blue) into a cavity photon (red) via the intermediate excitation of the NV center is suppressed in the $m_s = -1$ state by destructive quantum interference when $\delta_L = \Delta + \delta_C/2$.

photon into the cavity mode or vice versa [Fig. 2(b)]. The off-resonant coupling is the main distinguishing feature from resonant schemes which are limited by spontaneous emission [12]. The proposed two-qubit coupling mechanism relies on a spin-dependent scattering of laser photons into the cavity and back, which is possible because of the difference in zero-field splittings in the GS and ES. More specifically, the $m_s = 0$ and $m_s = -1$ states in the ES are not degenerate at B_0 , which leads to unequal scattering matrix elements for the $m_s = 0$ and $m_s = -1$ states. To produce an entangling quantum gate between two NV spin qubits, we find it to be sufficient if the laser-cavity photon scattering rate is different for the two spin states. If two NV centers are simultaneously coupling in this way to the same cavity mode, they will exchange a virtual cavity photon, thus generating a conditional phase shift; once the accumulated relative phase amounts to π , a CPHASE gate on the two NV spin qubits has been achieved.

In contrast to cavity-mediated spin interactions proposed for semiconductor quantum dots [13] where the spin-orbit splitting in the valence band can be used for spin-selective excitation with polarized radiation and Raman-type spin-flip transitions, we propose here to use another mechanism based on the different zero-field splittings of the NV ground and excited states to perform phase and controlled-phase operations. Earlier work on cavity-mediated quantum gates for defect qubits in diamond makes use of spectral hole burning [14] or a series of Λ systems [15]. The latter requires a sequence of at least three two-color pulses, while our scheme manages on just one single-color laser pulse for a CPHASE gate. A model for three NV centers coupled to a whispering gallery mode in a silica microsphere cavity using polarized excitation has been studied with the goal of achieving a three-qubit CPHASE gate [16]. Our scheme relies on spectral selectivity and thus does not require polarized excitation. The effect studied here produces an elementary, universal two-qubit CPHASE gate.

II. SINGLE NV CENTER IN A CAVITY

The NV center in its GS and ES spin triplet will be described by the Hamiltonian

$$H_{\text{NV}} = g_e \mu_B B S_z + \begin{pmatrix} E_g + D_{\text{es}} S_z^2 & g_L^* e^{-it\omega_L} \\ g_L e^{it\omega_L} & D_{\text{gs}} S_z^2 \end{pmatrix}, \quad (1)$$

where the first term describes the Zeeman splitting of the spin $\mathbf{S} = (S_x, S_y, S_z)$ with eigenvalues $m_s = -1, 0, 1$ in a magnetic field applied along the NV (z) axis with identical electronic Landé g factors g_e for the GS and ES (μ_B denotes the Bohr magneton). See Appendix A for a discussion of a possible magnetic-field misalignment. The second term in Eq. (1) includes the GS-ES energy gap $E_g = 1.945$ eV and the distinct GS and ES zero-field spin splittings $D_{\text{gs}} = 2.88$ GHz and $D_{\text{es}} = 1.44$ GHz. The off-diagonal terms describe laser excitation at a frequency ω_L , with the spin-independent dipole matrix element g_L . We assume that the ES orbital-state energies are strongly split by the strain in the diamond crystal, and we can concentrate on one of the two orbital ES triplets. The prerequisite for this to be a reasonable approximation is that the strain splitting exceeds the ES spin-orbit coupling $\lambda = 5.3$ GHz. Strain splittings in excess of this value and up to 20 GHz have been observed [17,18]. Taking only one orbital ES into account, we can view the Hamiltonian H_{NV} in Eq. (1) as a 6×6 matrix consisting of four 3×3 blocks. The Zeeman splitting described by the first term in Eq. (1) is independent of the orbital state. Using Pauli matrices τ_i to describe the GS-ES orbital state, i.e., $\tau_z = -1$ for the GS and $\tau_z = +1$ for the ES, and working in a rotating frame with the frequency ω_L , we can write

$$H_{\text{NV}} = g \mu_B B S_z + D S_z^2 - \frac{\Delta}{2} S_z^2 \tau_z + \frac{\delta_L}{2} \tau_z + g_L \tau_- + g_L^* \tau_+, \quad (2)$$

where $D = (D_{\text{gs}} + D_{\text{es}})/2 = 2.16$ GHz and $\Delta = D_{\text{gs}} - D_{\text{es}} = 1.44$ GHz denote the mean and difference between the GS and ES zero-field splittings, $\tau_{\pm} = (\tau_x \pm i\tau_y)/2$ describe transitions between the GS and ES, and $\delta_L = E_g - \omega_L$ is the laser detuning. We have so far neglected the spin-spin couplings in the ES but will discuss their effect further below.

We now consider a single NV center coupled to a near-resonant mode of a surrounding optical cavity which we describe, using the rotating-wave approximation, with the following Hamiltonian:

$$H = H_{\text{NV}} + \delta_C a^\dagger a + g_C (\tau_+ a + \tau_- a^\dagger), \quad (3)$$

where $\delta_C = \omega_C - \omega_L$ denotes the detuning of the cavity mode from the laser excitation frequency and a^\dagger (a) creates (annihilates) a cavity photon. The dipole matrix element g_C of the cavity field can be made real valued by an appropriate phase convention in the excited state. However, g_L cannot, in general, be made real valued at the same time; its phase ϕ depends on the phase of the laser field.

The magnetic field is chosen at a working point around the GS level crossing $B_0 = D_{\text{gs}}/g_e \mu_B$, where we focus our description on the nearly degenerate $m_s = -1$ and $m_s = 0$ levels (the $m_s = +1$ level will be included further below). This approximation is justified because the $m_s = +1$ level is

split off by the zero-field splitting, which is much larger than the spin-spin splittings coupling it to the other two spin levels. We describe here the situation of an initially empty cavity, which subsequently holds at most one virtual photon. Starting from an empty cavity and assuming sufficiently large detunings $\delta_C \gtrsim g_C$ and $\delta_L \gtrsim g_L$ of the cavity and laser frequencies, we can further reduce the relevant states to $|G0\rangle = |G, n=0\rangle$, $|G1\rangle = |G, n=1\rangle$, and $|E0\rangle = |E, n=0\rangle$, where G and E denote the GS and ES, respectively, and n denotes the cavity photon number. Including the two remaining spin projections, $m_s = -1, 0$ this leaves us with six states for a single NV and the cavity.

The combined action of the coupling to the laser and cavity fields can scatter a photon from the laser into the cavity or vice versa via an intermediate virtual ES. Starting from the Hamiltonian (3) and assuming that the electric dipole couplings $g_{L,C}$ are much smaller than the detuning from the one-photon resonances, we can derive an effective GS Hamiltonian for such second-order processes (see below),

$$\begin{aligned} \tilde{H} = & \delta_C a^\dagger a + \delta B |0\rangle\langle 0| \\ & + \sum_{m_s=0,-1} |m_s\rangle\langle m_s| (g_{m_s} a + g_{m_s}^* a^\dagger), \end{aligned} \quad (4)$$

where $|m_s\rangle\langle m_s|$ denotes the projection operator on the spin state with projection m_s ,

$$g_{m_s} = -g_L g_C \frac{\delta_L - \delta_C/2 + m_s \Delta}{(\delta_L + m_s \Delta)(\delta_L - \delta_C + m_s \Delta)} \quad (5)$$

is the effective coupling strength, and $\delta B = B - D_{gs}/g_e \mu_B$ is the magnetic-field detuning from the GS level crossing. The last term in Eq. (4) describes spin-dependent scattering processes at the NV center of a cavity photon into a laser photon or vice versa. Generally, we find that in order to construct a CPHASE gate, it is sufficient if $g_0 \neq g_{-1}$ (see also below). A possible extreme case where $g_0 = 0$ is described in Appendix B. In Eq. (4), we have suppressed optical Stark and Lamb shifts of order g_L^2 and g_C^2 , which will not play an essential role in what follows.

We now give a more detailed derivation of Eqs. (4) and (5), starting from Eq. (3). To describe the combined action of the coupling between the NV center and the laser and cavity fields we write Eq. (3) as $H = H_0 + V$ with the perturbation Hamiltonian

$$V = g_L \tau_- + g_L^* \tau_+ + g_C (\tau_+ a + \tau_- a^\dagger) \quad (6)$$

and eliminate the ES in order to derive an effective interaction using the Schrieffer-Wolff transformation [19,20],

$$H_{\text{eff}} = e^S H e^{-S} = H_0 + \frac{1}{2}[S, V] + \dots, \quad (7)$$

generated by the anti-Hermitian operator

$$\begin{aligned} S = & -g_L (\delta_L - \Delta + \Delta |0\rangle\langle 0|)^{-1} |G0\rangle\langle E0| \\ & - g_C (\delta_L - \delta_C - \Delta + \Delta |0\rangle\langle 0|)^{-1} |G1\rangle\langle E0| - \text{H.c.}, \end{aligned} \quad (8)$$

such that $[S, H_0] = -V$, and we obtain the effective GS interaction Hamiltonian

$$\tilde{H} = H_0 + \frac{1}{2}[S, V] \Big|_{\text{GS}}, \quad (9)$$

which directly leads to Eqs. (4) and (5).

III. TWO NV CENTERS COUPLED TO A COMMON CAVITY MODE

The scattering of a photon from the laser to the cavity field and vice versa, conditional on the spin (qubit) state of an NV center, can be used to construct a cavity-photon-mediated quantum gate between two NV spin qubits coupled to a common cavity mode. Starting from two NV centers ($i = 1, 2$), each coupled to the same cavity mode as described above (Fig. 1), we derive the effective coupling Hamiltonian for two NV spins by eliminating the virtual cavity photon.

It is important to recognize that the cavity-mediated interaction between the NV centers is a fourth-order process in the coupling strengths which prevents us from using the second-order Hamiltonian equation (4) directly to calculate the coupling between the NV center spins. In order to systematically account for all contributions up to the fourth order, we perform a fourth-order Schrieffer-Wolff transformation of the Hamiltonian describing two NV centers coupled to a common cavity mode,

$$\begin{aligned} H &= H_0 + H_{\text{int}}, \\ H_0 &= \delta_C a^\dagger a + \sum_{i=1,2} \left[\frac{1 + \tau_z^i}{2} (\delta_{Li} + \Delta S_{zi}) + \delta B_i S_{zi} \right], \\ H_{\text{int}} &= \sum_{i=1,2} (g_{Li} \tau_-^i + g_{Ci} a^\dagger \tau_-^i + \text{H.c.}), \end{aligned} \quad (10)$$

where we have restricted ourselves to the $S_z = 0$ and $S_z = -1$ states near the GS level crossing where $S_z^2 = -S_z$. As this Hamiltonian commutes with the operators S_{z1} and S_{z2} of the NV centers, we can treat it separately for each of the four ground-state spin configurations, which represent the logical basis for our two-qubit system. For each spin configuration, we consider the five states $|GG0\rangle$, $|GG1\rangle$, $|EG0\rangle$, $|GE0\rangle$, and $|EE0\rangle$, where $|X_1 X_2 n\rangle$ denotes the state with NV i ($i = 1, 2$) in the ground ($X_i = G$) or excited ($X_i = E$) state, while the cavity mode is occupied with n photons. In analogy with the previous section we are interested only in the effective interaction between the NV centers and the cavity in the NV ground state. To derive an effective spin Hamiltonian for the NV ground states, we decouple the two states $|GG0\rangle$ and $|GG1\rangle$ from the remaining three states by performing a Schrieffer-Wolff transformation [19,20]. In analogy with Eq. (7) and expanding to fourth order, we have

$$\begin{aligned} H_{\text{eff}} = & e^S H e^{-S} = H + [S, H] + \frac{1}{2}[S, [S, H]] \\ & + \frac{1}{6}[S, [S, [S, H]]] + \frac{1}{24}[S, [S, [S, [S, H]]]]. \end{aligned} \quad (11)$$

We then expand the matrix S as a series $S = S_1 + S_2 + S_3 + S_4 + \dots$, where each term S_i is derived using Eq. (11) under the requirement that there is no coupling between the $|GGn\rangle$ ($n = 0, 1$) subspace and the excited states of the NV centers up to i th order in the coupling constants g_L and g_C . In the sum (11), we then calculate all the residual terms and obtain the effective Hamiltonian in the basis

$|GG0\rangle, |GG1\rangle$,

$$H_{\text{eff}} = \begin{pmatrix} W_{GG0} + |\tilde{g}|^2/\delta_C & \tilde{g}^* \\ \tilde{g} & W_{GG1} - |\tilde{g}|^2/\delta_C \end{pmatrix}. \quad (12)$$

Introducing the phases ϕ_i of the lasers as $g_{Li} = |g_{Li}|e^{i\phi_i}$, we find for the eigenenergies of this effective Hamiltonian

$$W_{GG0} = \sum_{i=1,2} \left[\delta B_i m_{si} - \frac{|g_{Li}|^2}{\delta_{Li} + \Delta m_{si}} + \frac{|g_{Li}|^4}{(\delta_{Li} + \Delta m_{si})^3} - \frac{|g_{Li}|^2 |g_{Ci}|^2}{(\delta_{Li} + \Delta m_{si})^2 \delta_C} \right] - \frac{2|g_{L1}g_{L2}|g_{C1}g_{C2} \cos(\phi_1 - \phi_2)}{(\delta_{L1} + \Delta m_{s1})(\delta_{L2} + \Delta m_{s2})\delta_C} \quad (13)$$

and $W_{GG1} \approx \delta_C + \sum_{i=1,2} \delta B_i m_{si}$, whereas for the off-diagonal matrix element we obtain

$$\tilde{g} = - \sum_{i=1,2} \frac{e^{i\phi_i} g_{Ci} |g_{Li}| (\delta_{Li} + \Delta m_{si} - \delta_C/2)}{(\delta_{Li} + \Delta m_{si})(\delta_{Li} + \Delta m_{si} - \delta_C)}. \quad (14)$$

We present W_{GG0} only up to the fourth-order corrections, as only these terms will be important for the following discussion. We have also calculated W_{GG0} using conventional perturbation theory, rather than a Schrieffer-Wolff transformation, with identical results (see Appendix C). The expression for W_{GG0} in Eq. (13) consists of two parts, where each term of the first part depends on the spin state of only one NV center and thus leads only to single-qubit dynamics. Entanglement can be generated by the second part (last term) of Eq. (13),

$$\epsilon_{m_{s1}, m_{s2}} = - \frac{2|g_{L1}g_{L2}|g_{C1}g_{C2} \cos(\phi_1 - \phi_2)}{(\delta_{L1} + \Delta m_{s1})(\delta_{L2} + \Delta m_{s2})\delta_C}, \quad (15)$$

as it depends on the spin state of both NV centers. We note that these energy shifts consist of many fourth-order contributions. While some of these terms have the form $\sim g_{m_1} g_{m_2} / \delta_C$, the particular structure of the second-order scattering matrix element (5) does not appear after the summation of all terms.

Calculating this term for each spin configuration $|m_{s1}, m_{s2}\rangle = |-1, -1\rangle, |-1, 0\rangle, |0, -1\rangle, |0, 0\rangle$ leaves us with the diagonal spin Hamiltonian

$$H_{2q} = \begin{pmatrix} \epsilon_{-1,-1} & 0 & 0 & 0 \\ 0 & \epsilon_{-1,0} & 0 & 0 \\ 0 & 0 & \epsilon_{0,-1} & 0 \\ 0 & 0 & 0 & \epsilon_{0,0} \end{pmatrix}. \quad (16)$$

This Hamiltonian generates a quantum gate $\exp(-itH_{2q})$ which up to single-qubit operations is the CPHASE gate $U = \text{diag}(1, 1, 1, e^{i\gamma})$ with

$$\gamma = \frac{2|g_{L1}g_{L2}|g_{C1}g_{C2}\Delta^2 \cos(\phi_1 - \phi_2)}{\delta_C \delta_{L1} \delta_{L2} (\delta_{L1} - \Delta)(\delta_{L2} - \Delta)} t. \quad (17)$$

Equation (17) proves that the interaction of two NVs through the cavity can give rise to an entangling gate. This gate can be controlled both by the amplitude $|g_{Li}|$ and phase ϕ_i of the lasers and by the detuning of the laser frequency from the cavity mode δ_{Li} .

The results of this section can be considered only a qualitative proof of the entangling gate. They are valid as long as the perturbation analysis works, which implies that

the couplings g_{Li}, g_{Ci} are much smaller than the detunings δ_C, δ_{Li} . Moreover, to make predictions one should take into account the spin-spin interaction in the excited state of the NVs, which will be done in the next section in the description of our numerical results.

IV. SPIN-SPIN INTERACTION

To make quantitative predictions, we need to include the spin-spin interactions in the ES which have been studied both experimentally [17, 18, 21] and theoretically [22, 23],

$$H_s = \frac{1}{2}(1 + \tau_z) \left[\frac{\Delta_1}{2}(S_y^2 - S_x^2) + \frac{\Delta_2}{\sqrt{2}}(S_x S_z + S_z S_x) \right], \quad (18)$$

where $\Delta_1 = 1.55$ GHz and $\Delta_2 \simeq 0.15$ GHz.

The Hamiltonian of the system will then take the form

$$H = H_0 + H_{\text{int}} + H_s, \quad (19)$$

where H_0 and H_{int} were introduced in the previous section. In the spin Hamiltonian the Δ_1 term mixes the spin states $m_s = -1$ and $m_s = 1$, while the Δ_2 term mixes $m_s = -1$ and $m_s = 0$, as well as $m_s = 0$ and $m_s = 1$. Therefore, we can no longer treat each of the four logical states separately.

It is important to note that both cavity photon creation and spin-spin interaction are possible only when one of the NVs is in the excited state. To achieve this and thus create a quantum gate, laser excitation can be used to transform the initial ground state of the NVs. But it is also important that after the excitation is switched off, the system should remain in a final state that is the coherent superposition of the logical basis states. Thus, the probability of having an excited NV after the laser pulse is turned off should be very low. This will be the case if the intensity of the lasers changes slowly, such that the adiabatic theorem ensures that the system remains in the same eigenstate of the time-dependent Hamiltonian. The final state of the system after the pulse is turned off will correspond to the ground state of the NVs and zero-cavity photons, the logical basis of the two-qubit system.

We now introduce our numerical results obtained for this system, including spin-spin interactions. The laser detuning δ_L and the cavity detuning δ_C are assumed to be 1640 and 400 MHz, respectively. The distance between the ground state and the lower excited state of the NV is then $\delta_L - \Delta = 200$ MHz for an $m_s = -1$ spin state and $\delta_L = 1640$ MHz for an $m_s = 0$ spin state. The energy of the cavity excitation is $\delta_C = 400$ MHz. The inverses of these values (5, 0.6, 2.5 ns, respectively) define the internal dynamical rate of the system, with respect to which one has to choose the ramp time of the pulse. To stay within the adiabatic regime we took the pulse $g_L(t)$ to be a convolution of a rectangle and a Gaussian with a full width at half maximum (FWHM) of 133 ns and 20 ns, respectively. The coupling g_L at the maximum of the pulse is assumed to be $g_{L,\text{max}} = 24$ MHz. The coupling between the NV and the cavity is assumed to be $g_C = 100$ MHz. We consider both NVs to be identical and driven by two identical and synchronized lasers with the same amplitude, phase, and pulse form described above. Note that the two-qubit gate operation requires neither the NV centers nor the driving fields

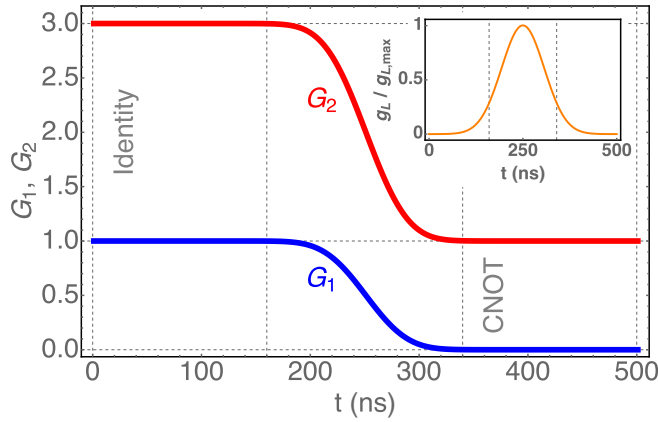


FIG. 3. Time dependence of the Makhlin invariants G_1 and G_2 during the operation of a cavity-mediated two-qubit gate. Before the lasers are turned on, $G_1 = 1$ and $G_2 = 3$, which corresponds to the identity operation. When the lasers are turned on, the two NVs start to interact through the cavity, which leads to the appearance of entanglement and change in Makhlin invariants. After the lasers are turned off, the final state of the system is related to the initial one by a CNOT operation, characterized by Makhlin invariants $G_1 = 0$ and $G_2 = 1$. The parameters chosen for this plot are $g_C = 100$ MHz, $\delta_C = 400$ MHz, $\delta_L = 1640$ MHz. Inset: Laser pulse shape with maximum $g_{L,\max} = 24$ MHz.

to be identical; this choice is made here only to simplify the analysis. Under these assumptions we numerically propagate each of the four logical states of the system. This results in a 4×4 unitary in the logical space of the two-qubit system, corresponding to a CNOT gate, as shown by the Makhlin invariants G_1 and G_2 (Fig. 3), for which the values 1 and 0, respectively, were obtained, which is a characteristic of a CNOT gate [24].

V. DISCUSSION

We have shown that virtual exchange of photons in an optical cavity can mediate the two-qubit CPHASE gate between two NV spin qubits in diamond. Combined with single-qubit operations, produced by rf excitation or by laser fields [25], the CPHASE gate allows for arbitrary (universal) quantum computations. Therefore, optical cavity QED with NV centers in diamond represents a realistic path towards spin-based quantum information processing. The cavity-mediated quantum gate proposed here could be applied to other defects with a similar level structure, i.e., comprising spin-triplet ground and excited states with deviating zero-field splittings. For example, we expect that the gate protocol would also work for certain divacancy centers in silicon carbide.

As a further prerequisite for the scheme to work, the NV spin coherence time and average time between cavity photon loss must be longer than the gate operation time $t \sim 200$ ns. The NV spin coherence time can reach $1/\gamma_2 = T_2 \sim 10 \mu\text{s}$, even at elevated temperatures. The photon loss rate can be estimated as $\tau^{-1} \sim (g/\delta_C)^2 \omega_C / 2\pi Q$, where $(g/\delta_C)^2 \sim 10^{-3}$ is the probability for the cavity mode to be occupied by a virtual photon during the gate operation and $\kappa = \omega_C / 2\pi Q$ is the photon loss rate in the cavity with quality factor Q . For the

parameters used above, a Q factor of $Q \sim 10^5$ is needed to achieve $\tau \sim 200$ ns. Because $\tau \sim \delta_C^2$ while $t \sim 1/g_{12} \sim \delta_C$, increasing the detuning δ_C allows the use of cavities with lower Q at the expense of slower gates, which in turn are admissible for sufficiently long T_2 . The limit of this scaling can be described in terms of a (coherent) cooperativity factor [26] $C_2 = g/\sqrt{\kappa\gamma_2} \gg 1$.

Finally, we expect this scheme to work below a temperature of about 20 K, where the excited-state levels are stable. It is an open question whether a variation of this scheme would also work at higher temperatures.

In a scalable qubit architecture, pairs of qubits need to be selectively coupled within a large array. A possible architecture comprises single NV centers in optical cavities linked via optical fibers [27]. The coupling mechanism described here lends itself to another architecture where many NV centers are embedded in a single cavity. In an array with separations between NV centers on the order of 10 to 100 nm, selective pairwise coupling can be accomplished with a combination of spatial and spectral selectivity of the laser excitation.

ACKNOWLEDGMENTS

We thank A. Auer, C. Chamberland, M. Lukin, and C. Yale for helpful discussions. We acknowledge funding from AFOSR and NSF (D.D.A.) and from Konstanz Center of Applied Photonics (CAP), German Research Foundation (DFG) Project No. SFB767, and BMBF Q.com-HL (G.B.).

APPENDIX A: MAGNETIC-FIELD ALIGNMENT

In our model, we have so far assumed that the magnetic field is perfectly aligned with the NV axis of both defects involved in the CPHASE gate. This raises two important issues: (1) how to treat NV centers with different orientations with respect to the diamond crystal and (2) the extent to which the CPHASE operation will be disturbed by any small misalignment of the magnetic field. As for point (1), we note that there are four distinct NV orientations (up to small misalignments which we discuss below). Only NV centers with their orientation along the external B field will be near resonance and will participate in the CPHASE gate operation, while the NV centers oriented along the three other axes can be safely ignored. Regarding point (2), the field misalignment will add a term $g\mu_B B_x S_x$ to the Hamiltonian equation (1), where $B_x = B \tan \phi \approx B\phi$ is the transverse (misalignment) field (chosen to point in the x direction) and $\phi \ll 1$ denotes the misalignment angle. The effect of the misalignment field is small if $B_x \ll \delta B$. For a misalignment of 1° , the NV center should be operated at least $\delta B \approx 20$ G away from the level anticrossing.

APPENDIX B: MINIMAL MODEL FOR SPIN-DEPENDENT LASER-CAVITY PHOTON SCATTERING

Here, we provide a minimal model to explain the spin-dependent cancellation of laser-cavity photon scattering. Neglecting spin-spin coupling and assuming g_L and g_C to be real, we can treat the two spin states $m_S = 0$ and $m_S = -1$

separately, with the Hamiltonian

$$H(m_S) = \begin{pmatrix} 0 & 0 & g_L \\ 0 & \delta_C & g_C \\ g_L & g_C & \delta_L + m_S \Delta \end{pmatrix}, \quad (\text{B1})$$

in the basis $|G0\rangle, |G1\rangle, |E0\rangle$. For simplicity, we choose $\delta_L = \Delta + \delta_C/2$ and find for the $m_S = -1$ state

$$H(m_S = -1) = \begin{pmatrix} 0 & 0 & g_L \\ 0 & \delta_C & g_C \\ g_L & g_C & \delta_C/2 \end{pmatrix}. \quad (\text{B2})$$

Note that in the rotating frame, the excited state now lies exactly in between the states with zero and one cavity photons. We introduce the dressed states $|\tilde{X}\rangle = e^S|X\rangle$,

$$\begin{aligned} |\tilde{G}0\rangle &= \left(1 - \frac{2g_L^2}{\delta_C^2}\right)|G0\rangle + \frac{2g_C g_L}{\delta_C^2}|G1\rangle - \frac{2g_L}{\delta_C}|E0\rangle, \\ |\tilde{G}1\rangle &= \left(1 - \frac{2g_C^2}{\delta_C^2}\right)|G1\rangle + \frac{2g_C g_L}{\delta_C^2}|G0\rangle + \frac{2g_C}{\delta_C}|E0\rangle, \\ |\tilde{E}0\rangle &= \left(1 - 2\frac{g_L^2 + g_C^2}{\delta_C^2}\right)|E0\rangle + \frac{2g_L}{\delta_C}|G0\rangle - \frac{2g_C}{\delta_C}|G1\rangle, \end{aligned}$$

and note that up to corrections cubic in $g_{L,C}/\delta_C$ they form an orthonormal basis of the space spanned by $|G0\rangle, |G1\rangle$, and $|E0\rangle$. In this new basis, the Hamiltonian equation (B2) takes the form

$$\tilde{H}(m_S = -1) = \begin{pmatrix} -\frac{2g_L^2}{\delta_C} & 0 & 0 \\ 0 & \delta_C + \frac{2g_C^2}{\delta_C} & 0 \\ 0 & 0 & \frac{\delta_C}{2} - 2\frac{g_L^2 + g_C^2}{\delta_C} \end{pmatrix}. \quad (\text{B3})$$

Note that $\tilde{H}(m_S = -1)$ is diagonal only for $\delta_L = \Delta + \delta_C/2$, while for general δ_L we find an effective coupling between $|\tilde{G}0\rangle$ and $|\tilde{G}1\rangle$. The absence of any effective coupling between $|\tilde{G}0\rangle$ and $|\tilde{G}1\rangle$ in the $m_S = -1$ state for $\delta_L = \delta_C/2 + \Delta$ can be traced back to the equal and opposite contributions from coupling the excited state $|E0\rangle$ to the two states $|G0\rangle$ and $|G1\rangle$, which are symmetrically arranged in energy around $|E0\rangle$ in the rotating frame. In contrast to this result, we find for the $m_S = 0$ state that

$$\tilde{H}(m_S = 0) = \begin{pmatrix} -\frac{2g_L^2}{\delta_C + 2\Delta} & g & 0 \\ g & \delta_C + \frac{2g_C^2}{\delta_C - 2\Delta} & 0 \\ 0 & 0 & \delta \end{pmatrix}, \quad (\text{B4})$$

with a nonzero amplitude for emitting or absorbing a cavity photon,

$$g = \frac{g_L g_C}{\delta_C - 2\Delta} - \frac{g_L g_C}{\delta_C + 2\Delta} = \Delta \frac{g_L g_C}{(\delta_C/2)^2 - \Delta^2} \quad (\text{B5})$$

and

$$\delta = \frac{\delta_C}{2} + \frac{g_L^2}{\delta/2 + \Delta} - \frac{g_C^2}{\delta_C/2 - \Delta}. \quad (\text{B6})$$

Note that for $\Delta = 0$, the destructive interference of the two terms in Eq. (B5) leads to a decoupling, $g = 0$. For general δ_L and $\Delta \neq 0$, we find distinct values of g for $m_S = 0$ and

$m_S = -1$ and thus a spin-dependent scattering of photons between the laser and cavity modes.

Using our minimal model, we can also discuss the validity of the effective Hamiltonian derived using the Schrieffer-Wolff transformation. The realization of a quantum gate (CPHASE) operation leads to a time-dependent problem because the control lasers need to be switched on and off to perform the quantum gate. The Schrieffer-Wolff transformation and use of the obtained effective Hamiltonian for this time-dependent problem are appropriate if the following two conditions are satisfied: (i) weak coupling (also mentioned in the main text), more specifically, $g_{L,C}, g \ll \delta_C$, and (ii) adiabatic switching on and off of the laser fields (sufficiently long ramp time τ_L) compared to the separation of ground and excited states (for $m_S = -1$ in the rotating frame), $\tau_L \gtrsim \hbar/\Delta$.

APPENDIX C: PERTURBATION ANALYSIS

In this Appendix we will give an alternative derivation of Eq. (13), using conventional time-independent perturbation theory. We are interested in the shift of the ground state of H_0 , induced by the perturbation H_{int} . The matrix element of H_{int} , which causes the transition from the initial state $|i\rangle$ to the final state $|f\rangle$, is

$$H_{\text{int}}^{i \rightarrow f} = \langle f | H_{\text{int}} | i \rangle. \quad (\text{C1})$$

Thus, the matrix elements of the perturbation are

$$H_{\text{int}}^{GG0 \rightarrow EG0} = H_{\text{int}}^{GE0 \rightarrow EE0} = g_{L1}, \quad (\text{C2})$$

$$H_{\text{int}}^{GG0 \rightarrow GE0} = H_{\text{int}}^{EG0 \rightarrow EE0} = g_{L2}, \quad (\text{C3})$$

which account for the interaction between the NV centers and the laser, and

$$H_{\text{int}}^{EG0 \rightarrow GG1} = g_{C1}, \quad (\text{C4})$$

$$H_{\text{int}}^{GE0 \rightarrow GG1} = g_{C2}, \quad (\text{C5})$$

which account for the interaction between the NV centers and the cavity. There are also six inverse transitions with the conjugate matrix elements. We consider only the first five energy levels of H_0 , as we use fourth-order perturbation theory and higher-energy levels are not excited under this approximation.

One can think of the perturbation to the particular eigenenergy level of H_0 as arising from transitions that start and end at this level. First-order processes are thus absent as we have no diagonal terms in the perturbation. The second-order processes are

$$|GG0\rangle \mapsto |EG0\rangle \mapsto |GG0\rangle, \quad (\text{C6})$$

$$|GG0\rangle \mapsto |GE0\rangle \mapsto |GG0\rangle, \quad (\text{C7})$$

and the second-order energy correction will be

$$\delta E_2 = -\frac{|g_{L1}|^2}{\delta_{L1} + \Delta m_{S1}} - \frac{|g_{L2}|^2}{\delta_{L2} + \Delta m_{S2}}. \quad (\text{C8})$$

There are no third-order processes that would start and end in the ground state, and therefore, the third-order correction

to the energy is zero. Now we include all of the fourth-order processes, described by the formula

$$\delta E_4 = - \sum_{i,j,k \neq GG0} \frac{H_{\text{int}}^{GG0 \rightarrow i} H_{\text{int}}^{i \rightarrow j} H_{\text{int}}^{j \rightarrow k} H_{\text{int}}^{k \rightarrow GG0}}{\langle i | H_0 | i \rangle \langle j | H_0 | j \rangle \langle k | H_0 | k \rangle} - \delta E_2 \sum_{i \neq GG0} \frac{H_{\text{int}}^{GG0 \rightarrow i} H_{\text{int}}^{i \rightarrow GG0}}{\langle i | H_0 | i \rangle^2}, \quad (\text{C9})$$

where we have used that the orbital energy of the state $|GG0\rangle$ can be set to zero. Also, we have omitted all the terms that contain the diagonal perturbation elements, as those are zero for our system. The first term in this equation contains all eight fourth-order processes that exist for this system. The second term is responsible for renormalization of the perturbed wave function. After the calculation, we find

$$\delta E_4 = \frac{|g_{L1}|^4}{(\delta_{L1} + \Delta m_{s1})^3} + \frac{|g_{L2}|^4}{(\delta_{L2} + \Delta m_{s2})^3} - \frac{|g_{L1}|^2 |g_{c1}|^2}{(\delta_{L1} + \Delta m_{s1})^2 \delta_c} - \frac{|g_{L2}|^2 |g_{c2}|^2}{(\delta_{L2} + \Delta m_{s2})^2 \delta_c} - \frac{2|g_{L1}g_{L2}g_{c1}g_{c2} \cos(\phi_1 - \phi_2)}{(\delta_{L1} + \Delta m_{s1})(\delta_{L2} + \Delta m_{s2})\delta_c}. \quad (\text{C10})$$

It can easily be seen that $\delta B_1 m_{s1} + \delta B_2 m_{s2} + \delta E_2 + \delta E_4$ coincides with the result (13) obtained in Sec. III.

APPENDIX D: MAKHLIN INVARIANTS

We are interested in producing a two-qubit gate (e.g., U_{CPHASE}) only up to single-qubit operations, i.e.,

$$U(t) = \exp(-2\pi i t H_{2q}) = (W_1 \otimes W_2) U_{\text{CPHASE}}(V_1 \otimes V_2), \quad (\text{D1})$$

with V_i and W_i being arbitrary single-qubit unitaries. To test whether $U(t)$ and U_{CPHASE} are equivalent in this sense, one can use two invariants (G_1, G_2) [24] of a two-qubit unitary U , defined as

$$G_1 = (\text{tr } m)^2 / 16 \det U, \quad (\text{D2})$$

$$G_2 = [(\text{tr } m)^2 - \text{tr}(m^2)] / 4 \det U, \quad (\text{D3})$$

where $m = U_B^T U_B$ and $U_B = Q^\dagger U Q$, with Q being the transformation into the Bell basis,

$$Q = \frac{1}{\sqrt{2}} \begin{pmatrix} 1 & 0 & 0 & i \\ 0 & i & 1 & 0 \\ 0 & i & -1 & 0 \\ 1 & 0 & 0 & -i \end{pmatrix}. \quad (\text{D4})$$

For the identity operation $U(0) = \mathbb{1}$, we find $G_1 = 1$, $G_2 = 3$, whereas the CPHASE gate lies in the same class as the CNOT gate, with $G_1 = 0$, $G_2 = 1$. Finding the latter values for G_1 and G_2 with $U(t)$ for some time $t > 0$ therefore proves that we have generated the CPHASE gate (and with this also the CNOT gate) up to single-qubit operations.

-
- [1] V. V. Dobrovitski, G. D. Fuchs, A. L. Falk, C. Santori, and D. D. Awschalom, Quantum control over single spins in diamond, *Annu. Rev. Condens. Matter Phys.* **4**, 23 (2013).
- [2] T. Gaebel, M. Domhan, I. Popa, C. Wittmann, P. Neumann, F. Jelezko, J. R. Rabeau, N. Stavrias, A. D. Greentree, S. Prawer, J. Meijer, J. Twamley, P. R. Hemmer, and J. Wrachtrup, Room-temperature coherent coupling of single spins in diamond, *Nat. Phys.* **2**, 408 (2006).
- [3] F. Dolde, I. Jakobi, B. Naydenov, N. Zhao, S. Pezzagna, C. Trautmann, J. Meijer, P. Neumann, F. Jelezko, and J. Wrachtrup, Room-temperature entanglement between single defect spins in diamond, *Nat. Phys.* **9**, 139 (2013).
- [4] W. Pfaff, T. H. Taminiau, L. Robledo, H. Bernien, M. Markham, D. J. Twitchen, and R. Hanson, Demonstration of entanglement-by-measurement of solid-state qubits, *Nat. Phys.* **9**, 29 (2012).
- [5] B. Hensen, H. Bernien, A. E. Dréau, A. Reiserer, N. Kalb, M. S. Blok, J. Ruitenber, R. F. L. Vermeulen, R. N. Schouten, C. Abellán, W. Amaya, V. Pruneri, M. W. Mitchell, M. Markham, D. J. Twitchen, D. Elkouss, S. Wehner, T. H. Taminiau, and R. Hanson, Loophole-free Bell inequality violation using electron spins separated by 1.3 kilometres, *Nature (London)* **526**, 682 (2015).
- [6] Y.-S. Park, A. K. Cook, and H. Wang, Cavity QED with diamond nanocrystals and silica microspheres, *Nano Lett.* **6**, 2075 (2006).
- [7] C. F. Wang, R. Hanson, D. D. Awschalom, E. L. Hu, R. Feygelson, J. Yang, and J. E. Butler, Fabrication and characterization of two-dimensional photonic crystal microcavities in nanocrystalline diamond, *Appl. Phys. Lett.* **91**, 201112 (2007).
- [8] A. Faraon, C. Santori, Z. Huang, V. M. Acosta, and R. G. Beausoleil, Coupling of Nitrogen-Vacancy Centers to Photonic Crystal Cavities in Monocrystalline Diamond, *Phys. Rev. Lett.* **109**, 033604 (2012).
- [9] J. Riedrich-Möller, L. Kipfstuhl, C. Hepp, E. Neu, C. Pauly, F. Mücklich, A. Baur, M. Wandt, S. Wolff, M. Fischer, S. Gsell, M. Schreck, and C. Becher, One- and two-dimensional photonic crystal microcavities in single crystal diamond, *Nat. Nanotechnol.* **7**, 69 (2012).
- [10] D. Englund, B. Shields, K. Rivoire, F. Hatami, J. Vučković, H. Park, and M. D. Lukin, Deterministic coupling of a silicon nitrogen vacancy center to a photonic crystal cavity, *Nano Lett.* **10**, 3922 (2010).
- [11] M. J. Burek, Y. Chu, M. S. Z. Liddy, P. Patel, J. Rochman, S. Meesala, W. Hong, Q. Quan, M. D. Lukin, and M. Lončar, High quality-factor optical nanocavities in bulk single-crystal diamond, *Nat. Commun.* **5**, 5718 (2014).
- [12] A. M. Zagoskin, J. R. Johansson, S. Ashhab, and F. Nori, Quantum information processing using frequency control of impurity spins in diamond, *Phys. Rev. B* **76**, 014122 (2007).
- [13] A. Imamoglu, D. D. Awschalom, G. Burkard, D. P. DiVincenzo, D. Loss, M. Sherwin, and A. Small, Quantum Information Processing Using Quantum Dot Spins and Cavity QED, *Phys. Rev. Lett.* **83**, 4204 (1999).
- [14] M. S. Shahriar, P. R. Hemmer, S. Lloyd, P. S. Bhatia, and A. E. Craig, Solid-state quantum computing using spectral holes, *Phys. Rev. A* **66**, 032301 (2002).
- [15] D. Solenov, S. E. Economou, and T. L. Reinecke, Two-qubit quantum gates for defect qubits in diamond and similar systems, *Phys. Rev. B* **88**, 161403(R) (2013).

- [16] W. L. Yang, Z. Q. Yin, Z. Y. Xu, M. Feng, and J. F. Du, One-step implementation of multiqubit conditional phase gating with nitrogen-vacancy centers coupled to a high-Q silica microsphere cavity, *Appl. Phys. Lett.* **96**, 241113 (2010).
- [17] A. Batalov, V. Jacques, F. Kaiser, P. Siyushev, P. Neumann, L. J. Rogers, R. L. McMurtrie, N. B. Manson, F. Jelezko, and J. Wrachtrup, Low Temperature Studies of the Excited-State Structure of Negatively Charged Nitrogen-Vacancy Color Centers in Diamond, *Phys. Rev. Lett.* **102**, 195506 (2009).
- [18] L. C. Bassett, F. J. Heremans, D. J. Christle, C. G. Yale, G. Burkard, B. B. Buckley, and D. D. Awschalom, Ultrafast optical control of orbital and spin dynamics in a solid-state defect, *Science* **345**, 1333 (2014).
- [19] R. Winkler, *Spin-Orbit Coupling Effects in Two-Dimensional Electron and Hole Systems* (Springer, Berlin, 2003).
- [20] S. Bravyi, D. P. DiVincenzo, and D. Loss, Schrieffer-Wolff transformation for quantum many-body systems, *Ann. Phys. (NY)* **326**, 2793 (2011).
- [21] G. D. Fuchs, V. V. Dobrovitski, R. Hanson, A. Batra, C. D. Weis, T. Schenkel, and D. D. Awschalom, Excited-State Spectroscopy Using Single Spin Manipulation in Diamond, *Phys. Rev. Lett.* **101**, 117601 (2008).
- [22] M. W. Doherty, N. B. Manson, P. Delaney, and L. C. L. Hollenberg, The negatively charged nitrogen-vacancy center in diamond: The electronic solution, *New J. Phys.* **13**, 025019 (2011).
- [23] J. Maze, A. Gali, E. Togan, Y. Chu, A. Trifonov, E. Kaxiras, and M. D. Lukin, Properties of nitrogen-vacancy centers in diamond: The group theoretic approach, *New J. Phys.* **13**, 025025 (2011).
- [24] Yu. Makhlin, Nonlocal properties of two-qubit gates and mixed states, and the optimization of quantum computations, *Quantum Inf. Process.* **1**, 243 (2002).
- [25] C. G. Yale, B. B. Buckley, D. J. Christle, G. Burkard, F. J. Heremans, L. C. Bassett, and D. D. Awschalom, All-optical control of a solid-state spin using coherent dark states, *Proc. Natl. Acad. Sci. USA* **110**, 7595 (2013).
- [26] S. Kolkowitz, A. C. Bleszynski Jayich, Q. P. Unterreithmeier, S. D. Bennett, P. Rabl, J. G. E. Harris, and M. D. Lukin, Coherent sensing of a mechanical resonator with a single-spin qubit, *Science* **335**, 1603 (2012).
- [27] K. Nemoto, M. Trupke, S. J. Devitt, A. M. Stephens, B. Scharfenberger, K. Buczak, T. Nöbauer, M. S. Everitt, J. Schmiedmayer, and W. J. Munro, Photonic Architecture for Scalable Quantum Information Processing in Diamond, *Phys. Rev. X* **4**, 031022 (2014).